

# Modeling the second wave of COVID-19 infections in France and Italy via a stochastic SEIR model

Cite as: Chaos **30**, 111101 (2020); <https://doi.org/10.1063/5.0015943>

Submitted: 31 May 2020 . Accepted: 07 October 2020 . Published Online: 02 November 2020

 **Davide Faranda**, and  **Tommaso Alberti**



[View Online](#)



[Export Citation](#)



[CrossMark](#)

## ARTICLES YOU MAY BE INTERESTED IN

### [Stochastic effects on the dynamics of an epidemic due to population subdivision](#)

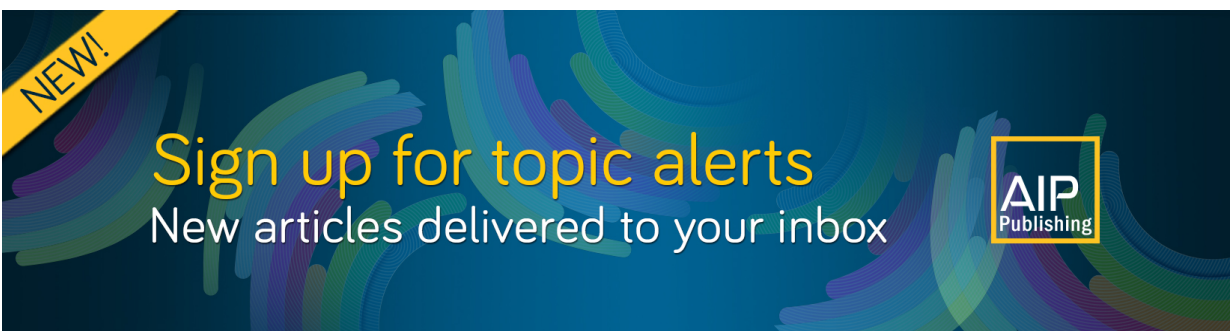
Chaos: An Interdisciplinary Journal of Nonlinear Science **30**, 101102 (2020); <https://doi.org/10.1063/5.0028972>

### [COVID-19 in the United States: Trajectories and second surge behavior](#)

Chaos: An Interdisciplinary Journal of Nonlinear Science **30**, 091102 (2020); <https://doi.org/10.1063/5.0024204>

### [Reconstructing regime-dependent causal relationships from observational time series](#)

Chaos: An Interdisciplinary Journal of Nonlinear Science **30**, 113115 (2020); <https://doi.org/10.1063/5.0020538>



# Modeling the second wave of COVID-19 infections in France and Italy via a stochastic SEIR model

Cite as: Chaos 30, 111101 (2020); doi: 10.1063/5.0015943

Submitted: 31 May 2020 · Accepted: 7 October 2020 ·

Published Online: 2 November 2020



Davide Faranda<sup>1,2,3,a)</sup> and Tommaso Alberti<sup>4</sup>

## AFFILIATIONS

<sup>1</sup>Laboratoire des Sciences du Climat et de l'Environnement, CEA Saclay l'Orme des Merisiers, UMR 8212 CEA-CNRS-UVSQ, Université Paris-Saclay & IPSL, 91191 Gif-sur-Yvette, France

<sup>2</sup>London Mathematical Laboratory, 8 Margravine Gardens, London W6 8RH, United Kingdom

<sup>3</sup>LMD/IPSL, Ecole Normale Supérieure, PSL Research University, 75005 Paris, France

<sup>4</sup>INAF—Istituto di Astrofisica e Planetologia Spaziali, Via del Fosso del Cavaliere 100, 00133 Roma, Italy

<sup>a)</sup>Author to whom correspondence should be addressed: [davide.faranda@lsce.ipsl.fr](mailto:davide.faranda@lsce.ipsl.fr)

## ABSTRACT

COVID-19 has forced quarantine measures in several countries across the world. These measures have proven to be effective in significantly reducing the prevalence of the virus. To date, no effective treatment or vaccine is available. In the effort of preserving both public health and the economical and social textures, France and Italy governments have partially released lockdown measures. Here, we extrapolate the long-term behavior of the epidemic in both countries using a susceptible-exposed-infected-recovered model, where parameters are stochastically perturbed with a lognormal distribution to handle the uncertainty in the estimates of COVID-19 prevalence and to simulate the presence of super-spreaders. Our results suggest that uncertainties in both parameters and initial conditions rapidly propagate in the model and can result in different outcomes of the epidemic leading or not to a second wave of infections. Furthermore, the presence of super-spreaders adds instability to the dynamics, making the control of the epidemic more difficult. Using actual knowledge, asymptotic estimates of COVID-19 prevalence can fluctuate of the order of  $10 \times 10^6$  units in both countries.

Published under license by AIP Publishing. <https://doi.org/10.1063/5.0015943>

**COVID-19 pandemic poses serious threats to public health as well as the economic and social stability of many countries. A real-time extrapolation of the evolution of COVID-19 epidemic is challenging both for the nonlinearities undermining the dynamics and for the ignorance of the initial conditions, i.e., the number of actual infected individuals. Here, we focus on France and Italy, which have partially released initial lockdown measures. The goal is to explore the sensitivity of COVID-19 epidemic evolution to the release of lockdown measures using dynamical [Susceptible-Exposed-Infected-Recovered (SEIR)] stochastic models. We show that the large uncertainties arising from both poor data quality and inadequate estimations of model parameters (incubation, infection, and recovery rates) propagate to long-term extrapolations of infection counts. Nonetheless, distinct scenarios can be clearly identified, showing either a second wave or a quasi-linear increase of total infections.**

## I. INTRODUCTION

SARS-CoV-2 is a zoonotic virus of the coronavirus family<sup>1</sup> that emerged in Wuhan (China) at the end of 2019<sup>2</sup> and rapidly propagated across the world until it has been declared a pandemic by the World Health Organization on March 11, 2020.<sup>3</sup> SARS-CoV-2 virus provokes an infectious disease known as COVID-19 that has an incredibly large spectrum of symptoms or none depending on the age, health status, and the immune defenses of each individual.<sup>4</sup> SARS-CoV-2 causes a potentially life-threatening form of pneumonia and/or cardiac injuries in a non-negligible patients fraction.<sup>5,6</sup>

To date, no treatment or vaccine is available for COVID-19.<sup>7</sup> Efforts to contain the virus and to not overwhelm intensive care facilities are based on quarantine measures, which have proven very effective in several countries.<sup>8–10</sup> These predictions were based on statistical and epidemiological models that, despite their simplicity,

well captured the growths of the epidemic.<sup>11–13</sup> Despite this, lockdown measures entail enormous economical, social, and psychological costs. Recent estimates of the International Monetary Fund recently announced a global recession that will drag global GDP lower by 3% in 2020, although continuously developing and changing as well as significantly depending on country to country.<sup>14</sup> More than  $20 \times 10^6$  people have lost their job in the United States,<sup>15</sup> and a large percentage of Italians have developed psychological disturbances such as insomnia or anxiety due to the strict lockdown measures.<sup>16</sup> Those measures have been taken on the basis of epidemic models, which are fitted on the available data.<sup>17</sup> In Italy, initial lockdown measures started on February 23 for 11 municipalities in both Lombardia and Veneto, which were identified as the two main Italian clusters. After the initial spread of the epidemic into different regions, all Italian territory was placed into a quarantine on March 9, with total lockdown measures, including all commercial activities (apart from supermarkets and pharmacies), non-essential businesses, and industries, and severe restrictions to transports and movements of people at regional, national, and international levels.<sup>18</sup> People were asked to stay at home or near for sporting activities and dog hygiene (within 200 m from home), to reduce as much as possible their movements (only for food shopping and care reasons), and smart-working was especially encouraged in both public and private administrations and companies. At the early stages of the epidemic, intensive cares were almost saturated with a peak of 4000 people on April 3 and a peak of hospitalizations of 30 000 on April 4, significantly reducing after these dates, reaching 1500 and 17 000, respectively, at the beginning of phase 2 on May 4, and 750 and 1000 on May 18 when lockdown measures on commercial activities were relaxed. These numbers, continuously declining during the next days and weeks, confirmed the benefit of lockdown measures.<sup>19</sup> Alarmed by the exponential growth of new infections and the saturation of the intensive care beds, also France introduced strict lockdown measures on March 17.<sup>20</sup> The French government restricted travel to food shopping, care, and work when teleworking was not possible, outings near home for individual sporting activity and/or dog hygiene, and it imposed the closure of the Schengen area borders as well as the postponement of the second round of municipal elections. The number of patients in intensive care, like the number of hospitalizations, overall peaked in early April and then started to decline, showing the benefits of lockdown measures. On Monday, May 11, France began a gradual easing of COVID-19 lockdown measures.<sup>21</sup> Trips of up to 100 km from home are allowed without justification, as will gatherings of up to ten people. Longer trips will still be allowed only for work or for compelling family reasons, as justified by a signed form. Guiding the government's plans for easing the lockdown is the division of the country into two zones, green and red, based on health indicators. Paris region (Ile de France), with about  $12 \times 10^6$  inhabitants is flagged, to date, as an orange zone.

In both countries, the release of lockdown measures has been authorized by authorities after consulting scientific committees, which were monitoring the behavior of the curve of infections using COVID-19 data. Those data are provided daily, following a request of the WHO. To date, the WHO guidelines require countries to report, at each day  $t$ , the total number of infected patients  $I(t)$  as well as the number of deaths  $D(t)$ . Large uncertainties have been

documented in the count of  $I(t)$ .<sup>22</sup> Whereas in the early stage of the epidemic several countries tested asymptomatic individuals to track back the infection chain, recent policies to estimate  $I(t)$  have changed. Most of the western countries have previously tested only patients displaying severe SARS-CoV-2 symptoms.<sup>23</sup> In an effort of tracking all the chain of infections, Italy and France are now testing all individuals displaying COVID-19 symptoms and those who had strict contacts with infected individuals. The importance of tracking asymptomatic patients has been proven in a recent study.<sup>24</sup> The authors have estimated that an enormous part of total infections were undocumented (80%–90%) and that those undetected infections were the source for 79% of documented cases in China. Tracking strategies have proven effective in supporting actions to reduce the rate of new infections, without the need for lockdown measures, as in South Korea.<sup>25</sup>

The goal of this paper is to explore possible future epidemic scenarios of the long-term behavior of the COVID-19 epidemic<sup>26</sup> but taking into account the role of uncertainties in both the parameter values and the infection counts to investigate different outcomes of the epidemic leading or not to a second wave of infections. To this purpose, we use a stochastic Susceptible-Exposed-Infected-Recovered (SEIR) model,<sup>27</sup> which consists in a set of ordinary differential equations, where control parameters are time-dependent and modeled via a stochastic process. This allows us to mimic the dependence on control parameters on some additional/external factors as super-spreaders<sup>28</sup> and the enforcing/relaxing of confinement measures.<sup>27</sup> As for the classical SEIR models<sup>29</sup> the population is divided into four compartmental groups, i.e., susceptible, exposed, infected, and recovered individuals. The stochastic SEIR model shows that long-term extrapolation is sensitive to both the initial conditions and the value of control parameters,<sup>27</sup> with asymptotic estimates fluctuating of the order of  $10 \times 10^6$  units in both countries, leading or not a second wave of infections. This sensitivity arising from both poor data quality and inadequate estimations of model parameters has also been recently investigated by means of a statistical model based on a generalized logistic distribution.<sup>30,31</sup> The paper is organized as follows: in Sec. II, we discuss the various sources of data for COVID-19 and their shortcomings, and then we discuss in detail the SEIR model and its statistical modeling. In Sec. III, we discuss the results focusing on the statistical sensitivity of the modeling and apply it to data from France and Italy. We finish, in Sec. IV, with some remarks and point out some limitations of our study.

## II. DATA AND MODELING

### A. Data

This paper relies on data stored into the Visual Dashboard repository of the Johns Hopkins University Center for Systems Science and Engineering (JHU CSSE) supported by ESRI Living Atlas Team and the Johns Hopkins University Applied Physics Lab (JHU APL). Data can be freely accessed and downloaded at <https://systems.jhu.edu/research/public-health/ncov/> and refer to the confirmed cases by means of a laboratory test.<sup>3</sup> Nevertheless, there are some inconsistencies between countries due to different protocols in testing patients (suspected symptoms, tracing-back procedures, wide range tests)<sup>32,33</sup> as well as to local management of

health infrastructures and institutions. As an example due to the regional-level system of Italian healthcare, data are collected at a regional level and then reported to the National level via the Protezione Civile transferring them to WHO. These processes could be affected by some inconsistencies and delays,<sup>34</sup> especially during the most critical phase of the epidemic diffusion that could introduce errors and biases into the daily data. These incongruities mostly affected the period between February 23 and March 10, particularly regarding the counts of deaths due to a protocol change from the Italian Ministry of Health.<sup>35</sup> A similar situation occurs in France where the initial testing strategy was based only on detecting those individuals experiencing severe COVID-19 symptoms.<sup>36</sup> In the post-lockdown phase, France has extended its testing capacity to asymptomatic individuals who have been in contact with infected patients.<sup>37</sup>

## B. A stochastic epidemiological susceptible-exposed-infected-recovered model

One of the most used epidemiological models is the so-called Susceptible-Exposed-Infected-Recovered (SEIR) model belonging to the class of compartmental models.<sup>29</sup> It assumes that the total population  $N$  can be divided into four classes of individuals that are susceptible  $S$ , exposed  $E$ , infected  $I$ , and recovered or dead  $R$  (assumed to be not susceptible to reinfection). The model is based on the following assumptions:

1. The total population does not vary in time, e.g.,  $dN/dt = dS/dt + dE/dt + dI/dt + dR/dt = 0, \forall t \geq 0$ ;
2. Susceptible individuals become infected that then can only recover or die, e.g.,  $S \rightarrow I \rightarrow R$ ;
3. Exposed individuals  $E$  encountered an infected person but are not yet themselves infectious;
4. Recovered or died individuals  $R$  are forever immune. Although the longevity of the antibody response is still unknown, it is known that antibodies to other coronaviruses wane over time, typically after 52 weeks from the onset of symptoms.<sup>38</sup> Concerning SARS-CoV-2, it has been shown that antibody levels may remain over the course of almost 2–3 months.<sup>39</sup> Nevertheless, not only antibodies are important for investigating immunity but also other immune cells named T cells play a crucial role in long-term immunity.<sup>40,41</sup> Recently, Kissler *et al.*<sup>42</sup> found that the duration of protective immunity may last 6–12 months. Our assumption seems, therefore, justified at least to study the dynamics of a second wave. We remark also that the basic SEIR model does not distinguish between immune and deaths and it cannot, therefore, be used to estimate the number of deceased people from COVID-19.

Thus, the model reads as

$$\frac{dS}{dt} = -\lambda S(t)I(t), \quad (1)$$

$$\frac{dE}{dt} = \lambda S(t)I(t) - \alpha E(t), \quad (2)$$

$$\frac{dI}{dt} = \alpha E(t) - \gamma I(t), \quad (3)$$

$$\frac{dR}{dt} = \gamma I(t), \quad (4)$$

where  $\gamma > 0$  is the recovery/death rate,  $\lambda = \lambda_0/S(0) > 0$  is the infection rate rescaled by the initial number of susceptible individuals  $S(0)$ , and  $\alpha$  is the inverse of the incubation period. Its discrete version can be simply obtained via an Euler scheme as

$$S(t+1) = S(t) - \lambda S(t)I(t), \quad (5)$$

$$E(t+1) = (1 - \alpha)E(t) + \lambda S(t)I(t), \quad (6)$$

$$I(t+1) = (1 - \gamma)I(t) + \alpha E(t), \quad (7)$$

$$R(t+1) = R(t) + \gamma I(t), \quad (8)$$

in which we fixed  $dt = 1$  day that is the time resolution of COVID-19 counts. By means of  $\gamma$  and  $\lambda_0$ , the model also allows us to derive the so-called  $R_0$  parameter, e.g.,  $R_0 = \lambda_0/\gamma$ , representing the average reproduction number of the virus. It is related to the number of cases that can potentially (on average) be caused by an infected individual during its infectious period ( $\tau_{inf} = \gamma^{-1}$ ). Early estimates in Wuhan<sup>43</sup> on January 2020 reported  $R_0 = 2.68^{2.86}_{2.47}$ , which led to  $\gamma = \gamma_0 = 0.37$  fixing  $\lambda \simeq 1$  as in Ref. 44 and a 95% confidence level range for the incubation period between 2 and 11 days.<sup>45</sup> Here, we set  $\alpha = \alpha_0 = 0.27$  (corresponding to an incubation period between 3 and 4 days). This value has been extracted as a median period in Ref. 45. However, the  $R_0$  parameter as well as model parameters  $\lambda, \gamma$ , and  $\alpha$  can vary in time during the epidemic due to different factors as the possible presence of the so-called super-spreaders,<sup>28</sup> intrinsic changes of the SARS-CoV-2 features, lockdown measures, asymptomatic individuals who are not tracked out, counting procedures and protocols, and so on.<sup>46</sup> The fact that all the timescales considered for the parameters are larger than one day also justifies the use of the discrete version of the model in Eqs. (5)–(8).

To deal with uncertainties in long-term extrapolations and with the time-dependency of control parameters, a stochastic approach could provide new insights into modeling epidemic,<sup>47–49</sup> especially when an epidemic shows a wide range of spatial and temporal variabilities.<sup>50–52</sup> However, instead of investigating how to get a realistic behavior by stochastically perturbing control parameters, here we investigate how uncertainties into the final counts  $C(t)$  are controlled by model parameters.<sup>27</sup> Thus, we use a stochastic version of the SEIR model in which the set of control parameters  $\kappa \in \{\alpha, \gamma, \lambda\}$  are extracted at each time step from random distributions. In the ordinary differential equation (ODE) model [Eqs. (1)–(4)], the introduction of stochastic terms corresponds to replacing  $\{\alpha, \gamma, \lambda\}$  with  $\{\alpha(t), \gamma(t), \lambda(t)\}$  and adding three more differential equations of the type

$$\frac{d\kappa}{dt} = -\kappa(t) + \kappa_0 + \varsigma_\kappa \xi(t), \quad (9)$$

where  $\kappa_0 \in \{\alpha_0, \gamma_0, \lambda_0\}$ ,  $\xi(t)$  is a random number extracted from a normal distribution for  $\alpha, \gamma$  and from a lognormal distribution for

$\lambda$  (see below). The stochastic model, therefore, reads as

$$dS = -\lambda(t)S(t)I(t) dt, \quad (10)$$

$$dE = [\lambda(t)S(t)I(t) - \alpha(t)E(t)] dt, \quad (11)$$

$$dI = [\alpha(t)E(t) - \gamma I(t)] dt, \quad (12)$$

$$dR = \gamma(t)I(t) dt, \quad (13)$$

$$d\lambda = \lambda_0 dt + \varsigma_\lambda dW(t), \quad (14)$$

$$d\alpha = \alpha_0 dt + \varsigma_\alpha dW(t), \quad (15)$$

$$d\gamma = \gamma_0 dt + \varsigma_\gamma dW(t), \quad (16)$$

where  $dW(t) = \xi(t) dt$  is the differential form of the Brownian motion. In order to test the stability of our model integrated with the Euler scheme (see MATLAB code in the [Appendix](#)), we perform 30 realizations of Eqs. (10)–(16) with the aforementioned parameters and initial conditions  $S(1) = 67 \times 10^6$  (French population),  $I(1) = 1$  and  $E(1) = R(1) = 0$ . We vary  $dt$  in the range  $0.1 < dt < 2$ . Results are displayed in [Fig. 1](#) in terms of daily infections  $I(t)$ . They show the typical bell-shaped curve of an epidemic wave. We get high stability of the integration when  $dt \leq 1$ . For larger values, the epidemic peak is first delayed ( $dt = 1.5$ ) and the model diverges (not shown) for  $dt = 2$ . In the following, we decide to stick to  $dt = 1$ , which will be convenient to compare our results with those released by the national health agencies as in both the countries, data are provided on a daily basis.

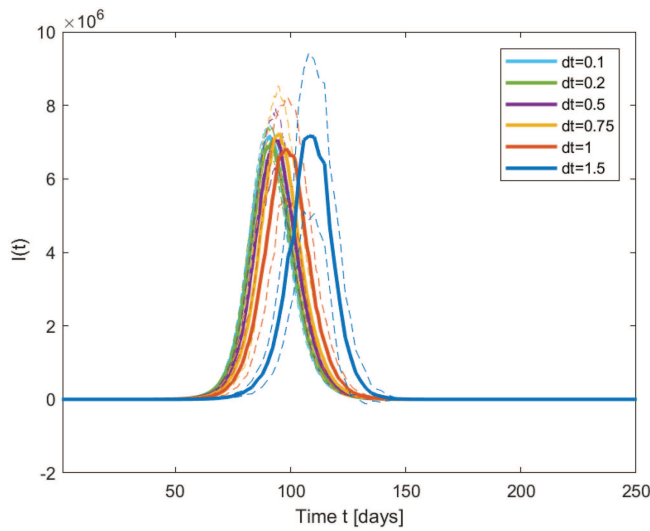


**FIG. 1.** Test of stability for the Susceptible-Exposed-Infected-Recovered (SEIR) model of COVID-19 for France [Eqs. (10)–(16)] with  $\lambda = 1/S(0)$ ,  $\alpha = 0.27$ , and  $\gamma = 0.37$ . Initial conditions are set to  $I(1) = 1$ ,  $S(1) = 6.7 \times 10^7$  (French population), and  $E(1) = R(1) = 0$ . The SEIR model is integrated with different  $0.1 < dt < 1.5$ . Solid lines show the average for 30 realizations of the SEIR stochastic models, and dotted lines extend to 1 SD of the mean.

With the choice of  $dt = 1$  day, one trivially gets that Eq. (9) is equivalent to sampling  $\alpha(t) \in \mathcal{N}(\alpha_0, \varsigma_\alpha^2; t)$ ,  $\gamma(t) \in \mathcal{N}(\gamma_0, \varsigma_\gamma^2; t)$  and

$$\log(\lambda(t)) \in \mathcal{N}(\log(\lambda_0 - \sigma^2/2), \sigma; t). \quad (17)$$

In this way, we can introduce instantaneous daily discrete jumps (e.g., take into account daily uncertainties) in the control parameters to properly model detection errors on infection counts, appropriately described through a discrete process<sup>53</sup> rather than a continuous one.<sup>54</sup> For  $\alpha$  and  $\gamma$ , we follow<sup>27</sup> and allow for Gaussian fluctuations of the parameters, with intensity  $\varsigma_\alpha = 0.2\alpha_0$  and  $\varsigma_\gamma = 0.2\gamma_0$ . These fluctuations simulate the range of uncertainties obtained in previous studies for the incubation time and the recovery time and discussed in Ref. 27. With respect to Ref. 27, we model the infection rate  $\lambda(t)$  using a lognormal distribution<sup>55</sup> to take into account the possible presence of super-spreaders, namely, individuals who can infect quickly a large number of susceptible people by having several strict social interactions.<sup>56</sup> Super-spreaders can be modeled by introducing heavy right tails for the distribution of  $\lambda$ . The location and the scale parameters chosen in Eq. (17) ensure that the mean of the distribution does not change, while  $\sigma$  is modified to explore super-spreaders influence. In the following, we will only consider three cases: (1)  $\sigma = 0.2$  for which the lognormal distribution tends to be symmetric and the fluctuations of  $\lambda$  are quasi-Gaussian around  $\lambda_0$  and (2)  $\sigma = 0.4$ , which models the effect of some possible super-spreaders and  $\sigma = 0.6$ , where several super-spreaders may be active at the same time.

### III. RESULTS

#### A. Model validation: First wave

We begin this section by validating the SEIR stochastic model on the first wave of infections. We have, therefore, to choose the initial conditions and then introduce the lockdown measures in the parameters.

##### 1. France

In France, the first documented case of COVID-19 infections goes back to December 27, 2019. Doctors at a hospital in the northern suburbs of Paris retested samples from patients between December 2, 2019 and January 16, 2020. Of the 14 patient samples retested, one sample from a 42-year-old man came back positive.<sup>57</sup> As an initial condition for the SEIR model, we, therefore, set  $I(t=1) = 1$  and  $t = 1$  corresponds to December 27, 2019. We then use  $R_0 = 2.68^{2,86}_{2,47}$ , which leads to  $\gamma = 0.37$  fixing  $\lambda_0 \simeq 1$ . Strict lockdown measures are introduced at  $t = 80$  (i.e., March 17, 2020). First-wave modeling results are shown in [Fig. 2](#). [Figure 2\(a\)](#) shows the modeled value of  $R_0$ . During confinement, we reduce the value of  $\lambda_0$  by a factor of 1/4. We base this new infection rate on the mobility data for France during confinement, which have shown a drop by  $\sim 75\%$  according to the INSERM report #11.<sup>58</sup> The resulting confinement  $R_0 \simeq 0.75$ , with an error in the range of values compatible with that published by the Pasteur Institute,<sup>59</sup> for all values of  $\sigma$  of the lognormal distribution of  $\lambda$  introduced [Eq. (17)]. The cumulative number of infections is shown in [Fig. 2\(b\)](#) and shows that, on average, between 6 and  $8 \times 10^6$  people have been infected by SARS-CoV-2 in France, depending on whether super-spreader effects are taken into account

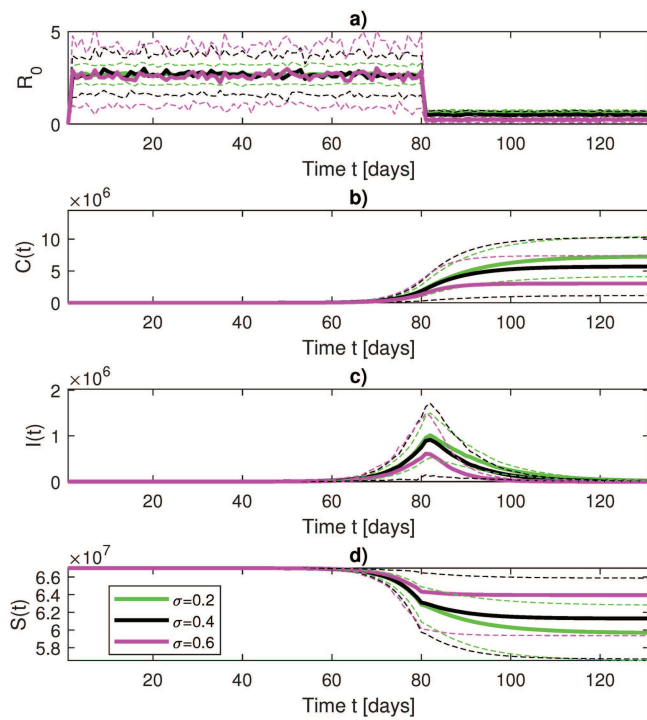


**FIG. 2.** Susceptible-Exposed-Infected-Recovered (SEIR) model of COVID-19 for France [Eqs. (10)–(16)] with  $\lambda = 1./S(0)$ ,  $\alpha = 0.27$ ,  $\gamma = 0.37$ , and  $dt = 1$ . Initial conditions are set to  $I(1) = 1$ ,  $S(1) = 6.7 \times 10^7$ , and  $E(1) = R(1) = 0$ .  $t = 1$  corresponds to December 27, 2019. Confinement is introduced at  $t = 78$  (March 17, 2020). Time evolution for (a) the basic reproduction number  $R_0$ , (b) the cumulative number of infections  $C(t)$ , (c) the daily infected individuals  $I(t)$ , and (d) the number of susceptible individuals  $S(t)$ . Solid lines show the average for 30 realizations of the SEIR stochastic models, and shadings extend to 1 SD of the mean. Colors represent different values of  $\sigma$  in the lognormal distribution of  $\lambda$  [Eq. (17)] from light to heavy tails.

via heavy tails in the distribution of  $\lambda$ . The uncertainty range is extremely large, according to the error propagation given by the stochastic fluctuations of the parameters (see Ref. 27 for explanations). It extends from a few hundred thousands of individuals up to  $15 \times 10^6$ . The error range is larger when super-spreaders are modeled. The average is, however, close to the value proposed by the authors in Ref. 60, who estimate a prevalence of  $\sim 6\%$  of COVID-19 in the French population. Another realistic feature of the model is the presence of an asymmetric behavior of the right tail of daily infections distributions [Fig. 2(c)] that has also been observed in real COVID-19 published data.<sup>61</sup>

## 2. Italy

For Italy, the first suspect COVID-19 case goes back to December 22, 2019, a 41-year-old woman who could only be tested positive for SARS-CoV-2 antibodies in April 2020.<sup>62</sup> As an initial condition, we, therefore, set  $I(t=1) = 1$  and  $t = 1$  corresponds to December 22, 2019. As for France, we use  $R_0 = 2.68^{2.86}_{2.47}$  leading to  $\gamma = 0.37$  if fixing  $\lambda_0 \simeq 1$ . A first semi-lockdown was set in Italy on March 9,

2020 ( $t = 78$ ) and enforced on March 22, 2020 ( $t = 89$ ). To simulate this two-step lockdown, we again base our reduction in  $R_0$  on the mobility data for Italy, which show for the first part of the confinement a reduction of about 50% and a similar reduction to France (75%) for the strict lockdown phase. Figure 3 shows the results for the first wave. The initial condition on susceptible individuals is fixed to  $S(1) = 6.0 \times 10^7$  corresponding to the estimate of the Italian population. A clear difference emerges with respect to the case of France in the behavior of  $R_0$ , which shows an intermediate reduction near  $t = 80$ , corresponding to March 11, 2020, to  $R_0 \simeq 1.4$  before reaching the final value of  $R_0 \simeq 0.7$ . This sort of “step” into the  $R_0$  time behavior corresponds to the time interval between semi- and full-lockdown measures, whose efficiency significantly increases after March 24, 2020, also corresponding to the peak value of infections. This is confirmed by looking at daily infection distributions [Fig. 3(c)] that shows a peak value near March 24, 2020, also observed in real COVID-19 data.<sup>30</sup> Note that, as for France, the magnitude of the fluctuations depends on the presence

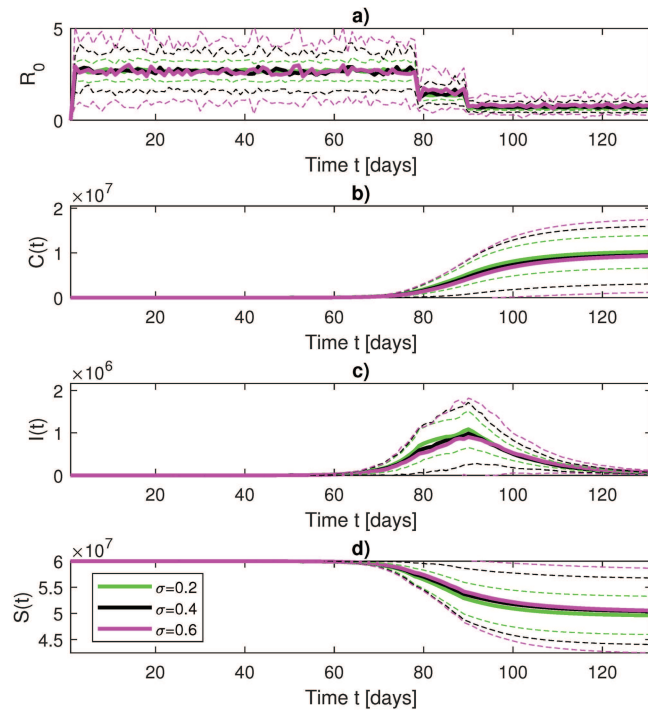


**FIG. 3.** Susceptible-Exposed-Infected-Recovered (SEIR) model of COVID-19 for Italy [Eqs. (10)–(16)] with  $\lambda = 1./S(0)$ ,  $\alpha = 0.27$ ,  $\gamma = 0.37$ , and  $dt = 1$ . Initial conditions are set to  $I(1) = 1$ ,  $S(1) = 6.0 \times 10^7$ , and  $E(1) = R(1) = 0$ .  $t = 1$  corresponds to December 22, 2019. First confinement measures are introduced at  $t = 80$  (March 9, 2020) and enforced at  $t = 89$  (March 22, 2020). Time evolution for (a) the basic reproduction number  $R_0$ , (b) the cumulative number of infections  $C(t)$ , (c) the daily infected individuals  $I(t)$ , and (d) the number of susceptible individuals  $S(t)$ . Solid lines show the average for 30 realizations of the SEIR stochastic models, and shadings extend to 1 SD of the mean. Colors represent different values of  $\sigma$  in the lognormal distribution of  $\lambda$  [Eq. (17)] from light to heavy tails.

of super-spreaders. The cumulative number of infections [Fig. 3(b)] shows that, on average, almost  $10 \times 10^6$  people have been infected by SARS-CoV-2 in Italy, ranging between a few hundred thousands up to  $15 \times 10^6$  due to the error propagation by the stochastic fluctuations of model parameters (see Ref. 27 for explanations), with the range depending on the presence of super-spreaders. Nevertheless, the wide range of uncertainty the average value is close to the value estimated from a team of experts of the Imperial College London according to which 9.6% of the Italian population has been infected, with a 95% confidence level ranging between 3.2% and 26%.<sup>63</sup> These

estimates correspond to cumulative infections of  $\sim 6 \times 10^6$ , ranging from  $\sim 2$  and  $\sim 16 \times 10^6$ , well in agreement with our model and other statistical estimates.<sup>64</sup>

## B. Future epidemic scenarios

After lockdown measures are released, for both countries, we model three different scenarios: a first one where all restrictions are lifted (back to normality), a second one where strict distancing

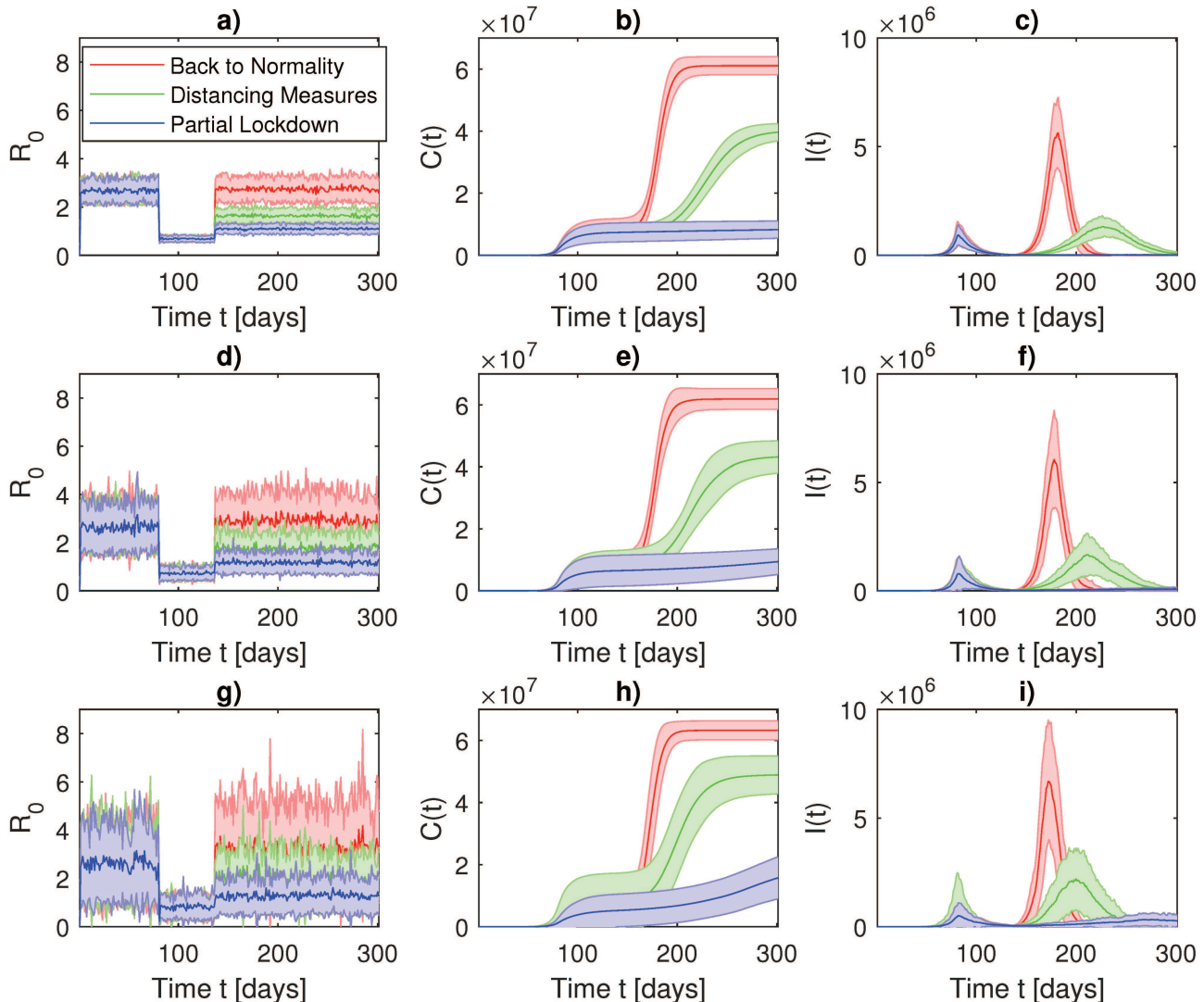


**FIG. 4.** Susceptible-Exposed-Infected-Recovered (SEIR) model of COVID-19 for the second wave in France. Initial conditions are set as in Fig. 2. After the confinement is released ( $t = 136$ , May 11, 2020), three scenarios are modeled: back to normality (red), distancing measures (green), and partial lockdown (blue). (a), (d), and (g) Time evolution for the basic reproduction number  $R_0$ . (b), (e), and (h) Time evolution for the cumulative number of infections  $C(t)$ . (c), (f), and (i) Time evolution for the daily infected individuals  $I(t)$ . (a)–(c)  $\sigma = 0.2$ , (d)–(f)  $\sigma = 0.4$ , and (g)–(i)  $\sigma = 0.6$  in the lognormal distribution for  $\lambda$  [Eq. (17)]. Solid lines show the average for 30 realizations of the SEIR stochastic models, and shadings extend to 1 SD of the mean.

measures are taken and a third one where the population remains mostly confined (partial lockdown).

### 1. France

Results for France are shown in Fig. 4. From top to bottom panels, we increase  $\sigma$  of the lognormal distribution [Eq. (17)] to model the presence of super-spreaders. Lockdown is released at  $t = 136$ , corresponding to May 11, 2020. The back to normality (red) scenario clearly shows a second wave of infections peaking in summer

(early July) and forcing group immunity in the French population. The distancing measures (green) scenario, corresponding to a reduction of the mobility of about 50%, leads to a second wave as intense as the first wave, but longer, at the end of August. As in the previous scenario, the distancing measures scenario allows us to reach a group immunity in France. A third partial lockdown scenario is modeled (blue). This latter scenario simulates an  $R_0 \simeq 1$ , which can be achieved by imposing strict distancing measures, partial lockdowns in cities with active clusters, and contact tracking. It results in a linear modest increase in the total number of infections

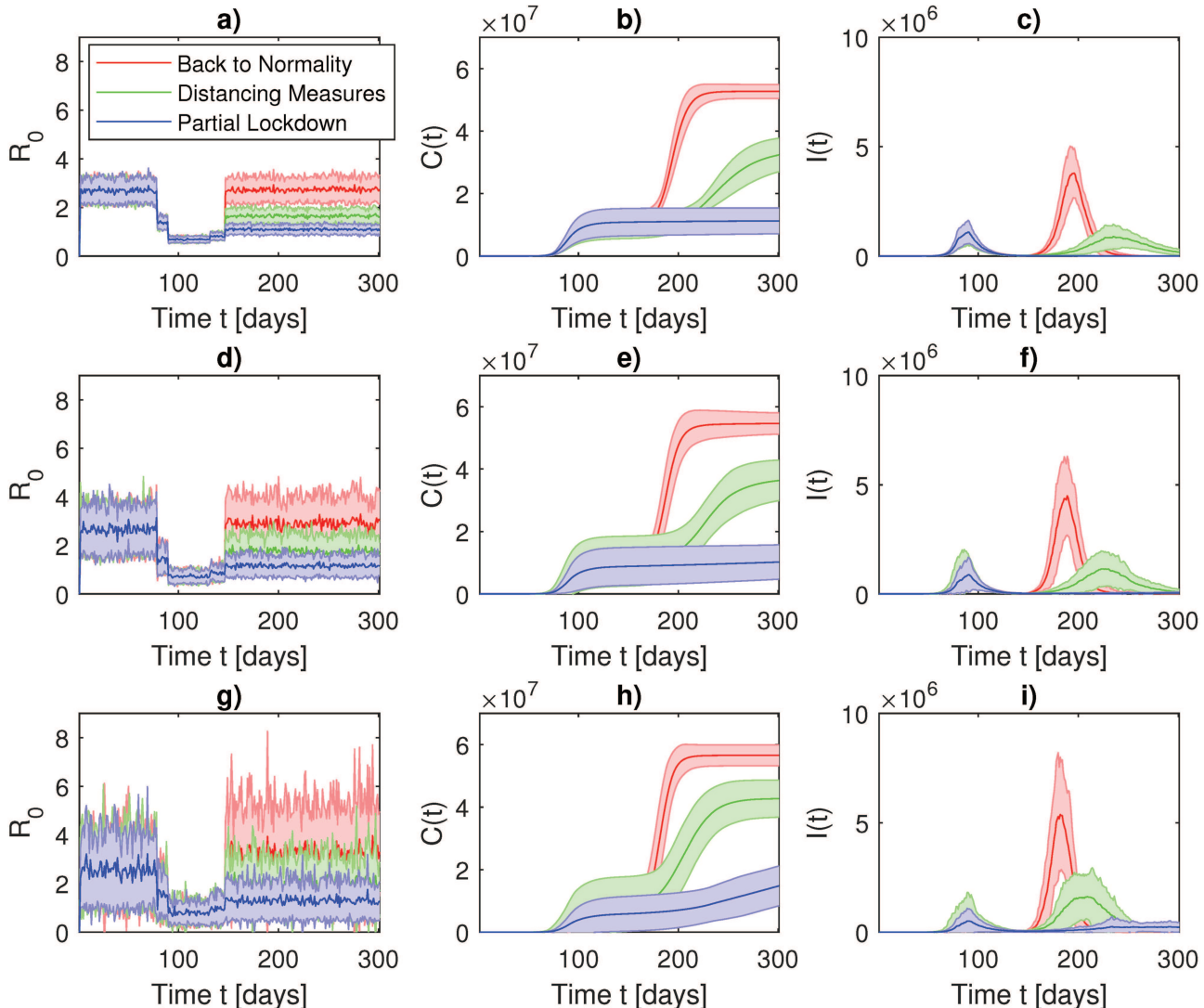


**FIG. 5.** Susceptible-Exposed-Infected-Recovered (SEIR) model of COVID-19 for the second wave in Italy. Initial conditions are set as in Fig. 3. After the confinement is released ( $t = 131$ , May 4, 2020 and  $t = 146$ , May 18, 2020), three scenarios are modeled: back to normality (red), distancing measures (green), and partial lockdown (blue). (a), (d), and (g) Time evolution for the basic reproduction number  $R_0$ . (b), (e), and (h) Time evolution for the cumulative number of infections  $C(t)$ . (c), (f), and (i) Time evolution for the daily infected individuals  $I(t)$ . (a)–(c)  $\sigma = 0.2$ , (d)–(f)  $\sigma = 0.4$ , and (g)–(i)  $\sigma = 0.6$  in the lognormal distribution for  $\lambda$  [Eq. (17)]. Solid lines show the average for 30 realizations of the SEIR stochastic models, and shadings extend to 1 SD of the mean.

that do not produce a proper wave of infections. As in the first-wave modeling, large uncertainties are also present in future scenarios although the three distinct behaviors clearly appear. Finally, the presence of super-spreaders may introduce additional difficulties in controlling partial lockdown scenarios. By comparing Figs. 4(b) and 4(h), we observe that super-spreaders can trigger an important growth of infections during positive fluctuations of  $R_0$  although its mean value is kept, by construction, constant. Another important effect of super-spreaders is to increase the uncertainty on the infection counts: error bars for  $\sigma = 0.6$  [Figs. 4(g)–4(i)] are two times wider than those for  $\sigma = 0.2$  [Figs. 4(a)–4(c)].

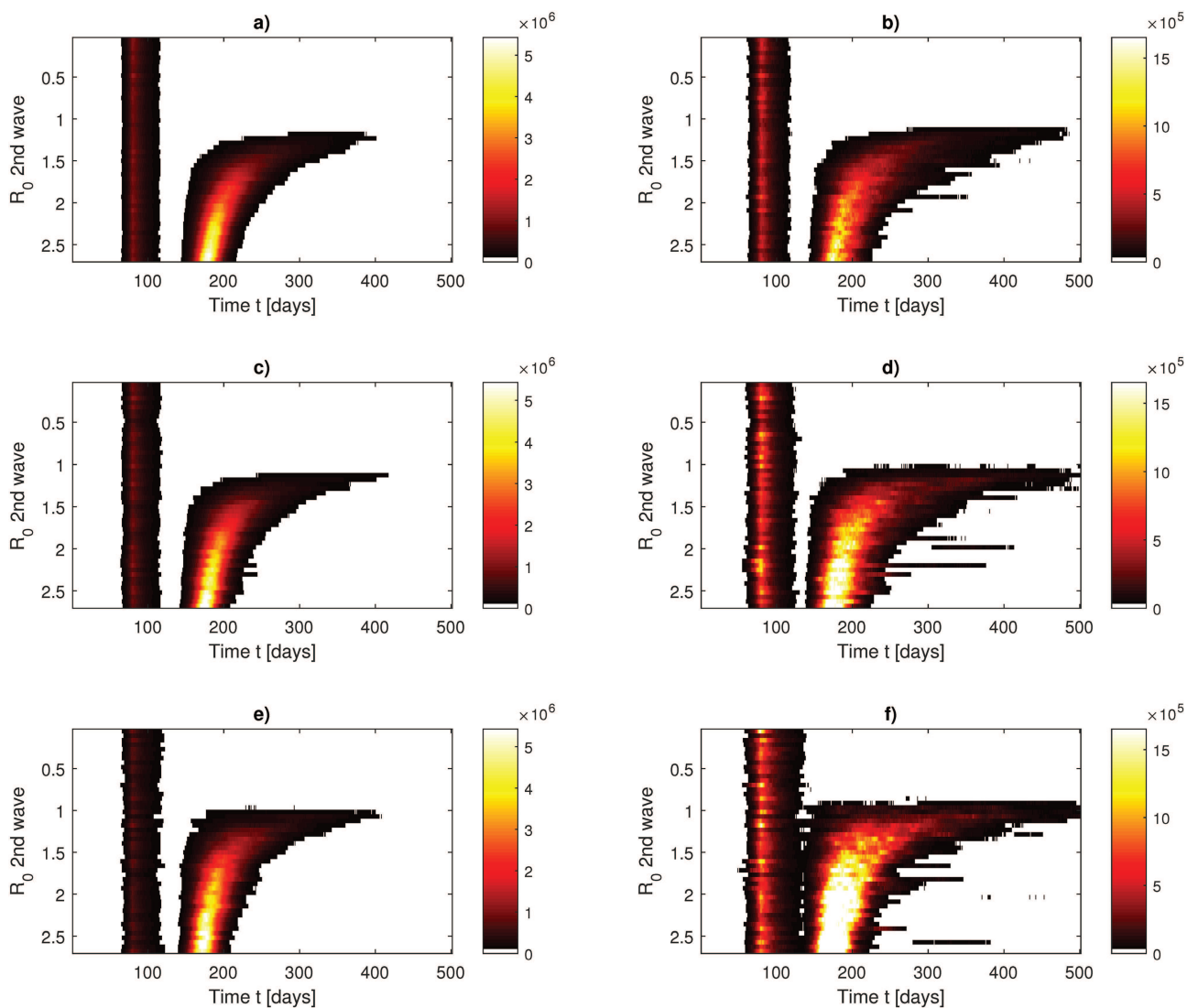


**FIG. 6.** Phase diagram for the Susceptible-Exposed-Infected-Recovered (SEIR) model of COVID-19 for the second wave in France. Initial conditions are set as in Fig. 2. After the confinement is released ( $t = 136$ , May 11, 2020) all possible  $R_0$  are modeled. (a), (c), and (e) Average of daily infected individuals  $l(t)$ . (b), (d), and (f) SD of daily infected individuals. Diagrams are obtained using 30 realizations of the SEIR models. (a) and (b)  $\sigma = 0.2$ , (c) and (d)  $\sigma = 0.4$ , and (e) and (f)  $\sigma = 0.6$  in the lognormal distribution for  $\lambda$  [Eq. (17)].

## 2. Italy

Figure 5 shows the results for modeling future epidemic scenarios for Italy. The first relaxation of lockdown measures started at  $t = 131$ , corresponding to May 4, 2020, while strict measures were finally released at  $t = 146$ , corresponding to May 18, 2020. The back to normality (red) scenario moves toward a second wave of infections whose peak occurs at  $t = 193$ , corresponding to July 4, 2020, exactly three months after initial lockdown measures were released (May 4, 2020). This would lead to the so-called herd immunity for the whole Italian population [see Fig. 5(b)], with a peak of daily infections near  $5 \times 10^6$  people [Fig. 5(c)], and  $R_0$  re-approaching

the initial value ( $R_0 = 2.68$ ). The distancing measures (green) scenario produces a second wave mostly similar, in terms of intensity, to the first wave, but occurring at  $t = 246$ , e.g., August 26, 2020. This scenario will lead to  $40 \times 10^6$  infected people, spanning between 25 and  $55 \times 10^6$ , thus producing a group immunity in Italy. A third scenario is modeled in which partial lockdown measures are taken (blue). This latter scenario leads to a more controlled evolution of cumulative infections, which still remain practically unchanged with respect to the first-wave cumulative number. It has been obtained by simulating an  $R_0 \simeq 1$ , resulting from strict distancing measures and reduced mobility, and does not produce a proper wave of

infections. However, all scenarios are clearly characterized by a wide range of uncertainties, although producing three well distinct behaviors in both cumulative and daily infections. The same conclusions made for France apply to Italy when it comes to the role of super-spreaders.

### C. Phase diagrams

In Sec. III B, we have seen that increasing  $R_0$  above 1 can or not produce a second wave of infections and introduce also a time delay in the appearance of a second wave of infections. We now analyze

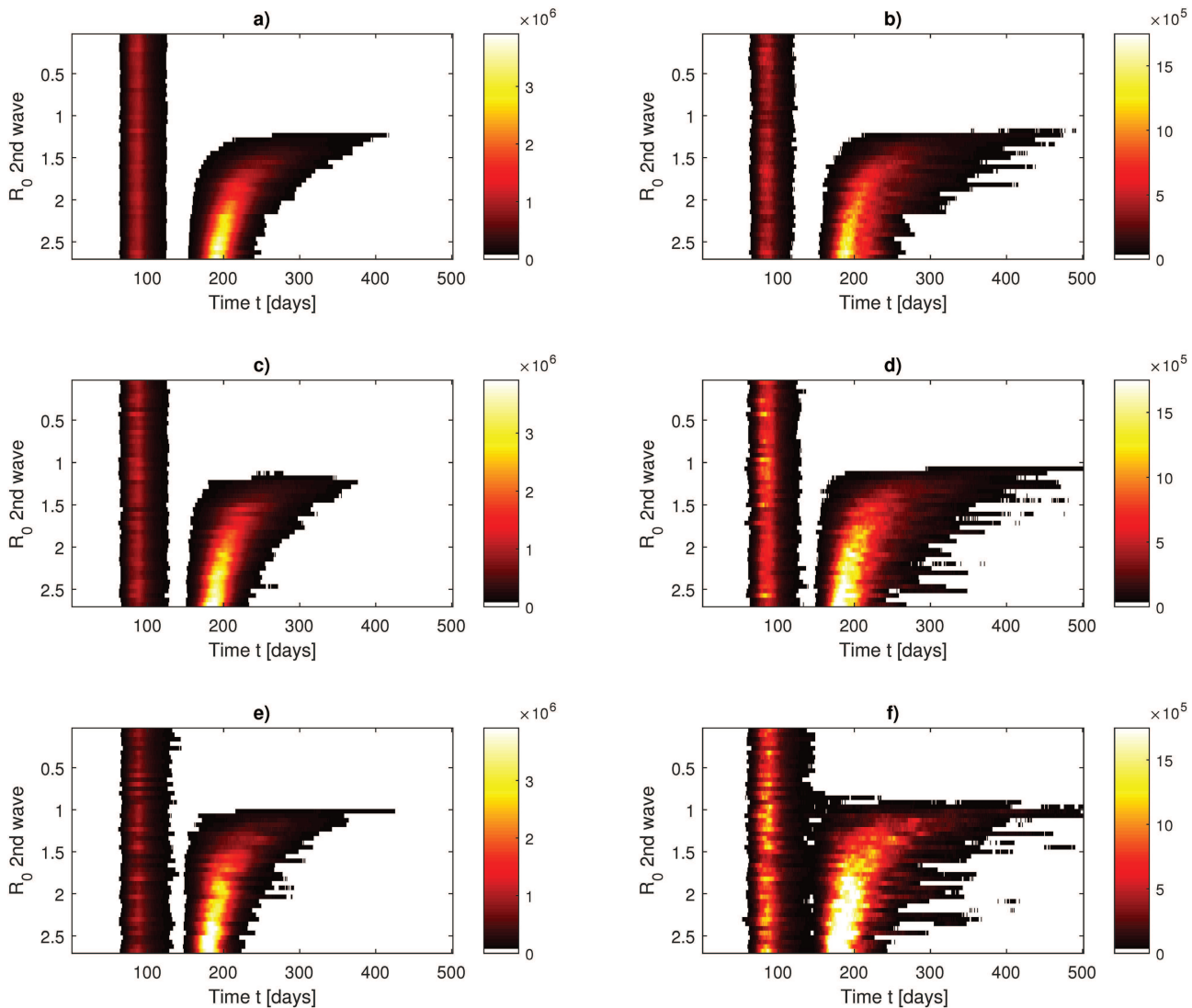


**FIG. 7.** Phase diagram for the Susceptible-Exposed-Infected-Recovered (SEIR) model of COVID-19 for the second wave in Italy. Initial conditions are set as in Fig. 3. After the confinement is released ( $t = 131$ , May 4, 2020 and then  $t = 146$  May 18, 2020) all possible  $R_0$  are modeled. (a), (c), and (e) Average of daily infected individuals  $l(t)$ . (b), (d), and (f) SD of daily infected individuals. Diagrams are obtained using 30 realizations of the SEIR models. (a) and (b)  $\sigma = 0.2$ , (c) and (d)  $\sigma = 0.4$ , and (e) and (f)  $\sigma = 0.6$  in the lognormal distribution for  $\lambda$  [Eq. (17)].

this effect in a complete phase diagram fashion. Phase diagrams are a standard tool used in statistical physics to visualize allowed and forbidden states for selected variables of complex systems and they have already been used in epidemiology.<sup>65</sup> Phase diagrams will help us to visualize for which values of  $R_0$  we will observe a second wave of infections. Figures 6 and 7 show the phase diagrams for France and for Italy, respectively. Panels (a) and (b) show the results for  $\sigma = 0.2$ , (c) and (d) for  $\sigma = 0.4$ , and (e) and (f) for  $\sigma = 0.6$ . The diagrams are built in terms of ensemble averages of the number of infections per day  $I(t)$  vs the average value of  $R_0$  after the confinement panels (a), and the errors [represented as SD of the average  $I(t)$  over the 30 realizations] are shown in panel (b). First, we note that despite some small differences in the delay of the COVID-19 second wave of infections peak, the diagrams are very similar. In order to avoid a second wave,  $R_0$  could fluctuate on values even slightly larger than one only if super-spreaders are not included. If super-spreaders are active, even small fluctuations of  $R_0 > 1$  can trigger a second wave. Furthermore, for  $1.5 < R_0 < 2$ , the second wave is delayed in Autumn or Winter 2020/2021 months. The uncertainty follows the same behavior as the average and it peaks when the number of daily infections is maximum. This means that the ability to control the outcome of the epidemic is significantly reduced if  $R_0$  is too high. The addition of super-spreaders also enhances the uncertainty in the infection counts, inducing large fluctuations, which might be difficult to control with partial lockdown measures.

#### IV. DISCUSSION

France and Italy have faced a long phase of lockdown with severe restrictions in mobility and social contacts. They have managed to reduce the number of daily COVID-19 infections drastically and released almost simultaneously lockdown measures. This paper addresses the possible future scenarios of COVID-19 infections in those countries by using one of the simplest possible models capable of reproducing the first wave of infections and to take into account uncertainties, namely, a stochastic SEIR model with fluctuating parameters.

We have first verified that the model is capable of reproducing the behavior of the first wave of infections and providing an estimate of the COVID-19 prevalence that is coherent with *a posteriori* estimates of the prevalence of the virus. The introduction of stochasticity accounts for the large uncertainties in both the initial conditions and the fluctuations in the basic reproduction number  $R_0$  originating from changes in virus characteristics, mobility, or misapplication in confinement measures. 30 realizations of the model have been produced and they show very different COVID-19 prevalence after the first wave. The range goes from thousands of infected to tens of millions of infections in both countries. Average values are compatible with those found in other studies,<sup>60,63</sup> whose aim was to estimate the prevalence of the virus. Nevertheless, we would like to stress that the corresponding number of infected people that was detected in France and Italy during the first wave was, according to the official released data, around 200 000 people. This discrepancy mostly comes from undetected cases, which can be a number many times bigger than the detected cases. The lower bound provided by the error bars of the realizations of the stochastic SEIR models is,

therefore, a limit for how many COVID-19 cases occurred in reality and it is at least as big as the number of detected cases for that period, for which data are available, plus the number of undetected cases, which can only be estimated.

Then, we have modeled future epidemic scenarios by choosing specific fluctuating behaviors for  $R_0$  and performing again 30 realizations of the stochastic SEIR model. Despite the very large uncertainties, distinct scenarios clearly appear from the noise. In particular, they suggest that a second wave can be avoided even with  $R_0$  values slightly larger than one. This means that actual distancing measures, which include the use of surgical masks, the reduction in mobility, and the active contact tracking can be effective in avoiding a second peak of infections without the need for imposing further strict lockdown measures. The analysis of phase diagrams shows that there is a sharp transition between observing or not a second wave of infections when the value of  $R_0$  is larger than 1 and that the exact value depends on the presence or not of super-spreaders. Moreover, the models show that the higher the  $R_0$  value, the lower the ability to control the number of infections in the epidemic. Similarly, if super-spreaders are particularly active, the infection counts are difficult to control and a second wave can be triggered more easily.

This model has also evident deficiencies in representing the COVID-19 infections. First of all, the choice of the initial conditions is conditioned by our ignorance of the diffusion of the virus in France and Italy in December 2019. Furthermore, we are unable to verify on an extensive dataset the outcome of the first wave: on the one hand, antibody blood tests still have a lower reliability,<sup>66</sup> and, on the other hand, they have not been applied on an extensive number of individuals to get reliable estimates. On top of the data-driven limitations, we have those introduced by the use of compartment models, as there are geographic, social, and age differences in the spread of the COVID-19 disease in both countries.<sup>21</sup> Furthermore, we also assume that fluctuations in the parameters of the SEIR model are Gaussian (for the incubation and recovery rate) or lognormal (for the infection rate), in order to simulate heavy tailed distributions;<sup>61,67</sup> however, the underlying (skewed) distribution is unknown. Another interesting research pathway is related to including the different psychological perceptions on the need for distancing measures depending, e.g., from the media coverage of the COVID-19 epidemic.<sup>68,69</sup> We would like to remark, however, that, to overcome these limitations, one would need to fit more complex models and introduce additional parameters which can, at the present stage, barely be inferred by the data.

Our choice to stick to the stochastic SEIR model is indeed driven by few factors: (1) despite its simplicity, our model allows for the possibility of modeling realistically the uncertainties with the stochastic fluctuations instead of adding new parameters whose inference may affect the results; (2) despite regional differences, national infection counts during the first wave have followed, for both France and Italy, a sigmoid function that could be modeled with the mean field SEIR model introduced in the present study; (3) unlike the UK or the US, both France and Italy have dealt with the epidemic with a national centralized approach: whenever intensive care facilities were saturating in one region, patients' transfers have been operated to other national hospitals; (4) lockdown measures have been applied uniformly on all the countries; and (5) introducing a spatial model also introduces several additional

parameters, namely, the interaction (exchange) coefficients among regions (at least  $20 \times 20$  coefficients for Italy and  $13 \times 13$  coefficients for France). The deficiencies of the COVID-19 testing capacities in many regions of both countries during the first phase prevent from having a reasonable estimation of the parameters, introducing uncontrollable errors. However, we acknowledge that, while the above mentioned factors were homogeneous across the different regions of France and Italy, the evolution of the epidemic was very heterogeneous between different regions and even departments in Italy and France, with certain departments having undergone saturation of the health care system (e.g., Lombardy and Bergamo, in particular, in Italy, or Strasburg and the Grand-Est region in France), and others remaining almost untouched by the epidemic. Moreover, geographical differences in Italy are present also in the measures after the removal of the lockdown, with masks being compulsory only in certain areas. There are, therefore, also several good reasons to go beyond the presented mean field SEIR models whenever high quality data will be available at a regional level.

This study can be applied to other countries, and this is why we publish the code of our analysis alongside the paper. To date, Northern Europe, UK, US, and other American countries are still facing the first wave of infections; so, future scenarios cannot be devised with the same clarity as those outlined in this study for France and Italy. Other studies are currently focusing on the second-wave modeling with different approaches. In Refs. 70–72, deterministic SIR models are employed to forecast the second wave of COVID-19 infections for Washtenaw County, Iran, and France. These models are extended to include other variables, which represent explicitly the number of patients taken to hospital or to intensive care units. However, their deterministic nature does not allow for propagating the uncertainty in the variables and, therefore, to get an estimate of the fluctuations in the number of hospitalized patients. In future studies, it could be interesting to add the kind of stochasticity suggested in the present study to the extended SIR models proposed by Refs. 70–72 in order to estimate the range of uncertainties for hospitals and intensive care units.

## ACKNOWLEDGMENTS

D.F. acknowledges all London Mathematical Laboratory fellows and B. Dubrulle, F. Pons, N. Bartolo, F. Daviaud, P. Yiou, M. Kagayema, S. Fromang, and G. Ramstein for useful discussions. T.A. acknowledges G. Consolini and M. Materassi for useful discussions.

## APPENDIX: NUMERICAL CODE

```
\% This appendix contains the MATLAB code
used to perform
\% the analysis contained in the paper via a
stochastic
\% SEIR model
\%\%VARIABLES INITIALIZATION
S=zeros(1,tmax);
E=zeros(1,tmax);
I=zeros(1,tmax);
R=zeros(1,tmax);
```

```
C=zeros(1,tmax);
\%\%PARAMETERS
\%\lambda Infection Rate is equal to 1
lambda0=1;
\% alpha is the inverse of the incubation
period (1/t_incubation)
alpha0=0.27;
\% R0 is equal to 2.68
R0=2.68;
\% gamma is the inverse of the mean infectious
period
gamma0=lambda0./R0;
\% INITIAL CONDITIONS
S(1)=67000000;
I(1)=1;
R(1)=0;
T(1)=0;
C(1)=0;
gamma(1)=gamma0;
alpha(1)=alpha0;
lambda(1)=lambda0./S(1);
\% EULER SCHEME FOR THE SDES
for t=1:1:tmax./dt
R0(t+1)=lambda(t)./gamma0;
T(t+1)=t.*dt^2;
S(t+1)=S(t)-(lambda(t).*S(t).*I(t)).*dt;
E(t+1)=E(t)+((lambda(t).*S(t).*I(t))-alpha(t)
.*E(t)).*dt;
I(t+1)=I(t)+(alpha(t).*E(t)-gamma(t).*I(t)).*dt;
R(t+1)=R(t)+(gamma(t).*I(t)).*dt;
lambda(t+1)=(lambda0*dt+lambda0./5*randn
.*sqrt(dt))./S(1);
gamma(t+1)=gamma0*dt+gamma0./5*randn
.*sqrt(dt);
alpha(t+1)=alpha0*dt+alpha0./5*randn
.*sqrt(dt);
\%cumulative infected
C(t+1)=gamma0.*sum(I);
end
```

## DATA AVAILABILITY

The data that support the findings of this study are openly available in <https://systems.jhu.edu/research/public-health/ncov/> at <https://systems.jhu.edu/research/public-health/ncov/>, maintained by Johns Hopkins University Center for Systems Science, Ref. 73. All figure scripts are available at <https://mycore.core-cloud.net/index.php/s/x8Wm4YyDVqEF2Xa>.

## REFERENCES

- <sup>1</sup>E. R. Gaunt, A. Hardie, E. C. Claas, P. Simmonds, and K. E. Templeton, “Epidemiology and clinical presentations of the four human coronaviruses 229E, HKU1, NL63, and OC43 detected over 3 years using a novel multiplex real-time PCR method,” *J. Clin. Microbiol.* **48**, 2940–2947 (2010).
- <sup>2</sup>J. Wu, W. Cai, D. Watkins, and J. Glanz, “How the virus got out,” *The New York Times*, 2020.
- <sup>3</sup>WHO, Coronavirus disease 2019 (COVID-19): Situation report, 2020, p. 51.

- <sup>4</sup>C. COVID and R. Team, "Severe outcomes among patients with coronavirus disease 2019 (COVID-19), United States, February 12–March 16, 2020," *MMWR Morb. Mortal Wkly Rep.* **69**, 343–346 (2020).
- <sup>5</sup>Y.-Y. Zheng, Y.-T. Ma, J.-Y. Zhang, and X. Xie, "COVID-19 and the cardiovascular system," *Nat. Rev. Cardiol.* **17**, 259–260 (2020).
- <sup>6</sup>C. Huang, Y. Wang, X. Li, L. Ren, J. Zhao, Y. Hu, L. Zhang, G. Fan, J. Xu, X. Gu *et al.*, "Clinical features of patients infected with 2019 novel coronavirus in Wuhan, China," *The Lancet* **395**, 497–506 (2020).
- <sup>7</sup>M. Cascella, M. Rajnik, A. Cuomo, S. C. Dulebohn, and R. Di Napoli, "Features, evaluation and treatment coronavirus (COVID-19)," in *Statpearls [Internet]* (StatPearls Publishing, 2020).
- <sup>8</sup>R. M. Anderson, H. Heesterbeek, D. Klinkenberg, and T. D. Hollingsworth, "How will country-based mitigation measures influence the course of the COVID-19 epidemic?," *The Lancet* **395**, 931–934 (2020).
- <sup>9</sup>M. Chinazzi, J. T. Davis, M. Ajelli, C. Gioannini, M. Litvinova, S. Merler, A. Pastore y Piontti, K. Mu, L. Rossi, K. Sun, C. Viboud, X. Xiong, H. Yu, M. E. Halloran, I. M. Longini, and A. Vespignani, "The effect of travel restrictions on the spread of the 2019 novel coronavirus (COVID-19) outbreak," *Science* **368**, 395–400 (2020).
- <sup>10</sup>H.-Y. Yuan, G. Han, H. Yuan, S. Pfeiffer, A. Mao, L. Wu, and D. Pfeiffer, "The importance of the timing of quarantine measures before symptom onset to prevent COVID-19 outbreaks—Illustrated by Hong Kong's intervention model," *medRxiv* 2020.05.03.20089482 (2020).
- <sup>11</sup>R. H. Mena, J. X. Velasco-Hernandez, N. B. Mantilla-Beniers, G. A. Carranco-Sapiens, L. Benet, D. Boyer, and I. P. Castillo, "Using the posterior predictive distribution to analyse epidemic models: COVID-19 in Mexico city," *arXiv:2005.02294* (2020).
- <sup>12</sup>S. Khajanchi and K. Sarkar, "Forecasting the daily and cumulative number of cases for the COVID-19 pandemic in India," *Chaos* **30**, 071101 (2020).
- <sup>13</sup>K. Sarkar, S. Khajanchi, and J. J. Nieto, "Modeling and forecasting the COVID-19 pandemic in India," *Chaos Soliton. Fract.* **139**, 110049 (2020).
- <sup>14</sup>N. Fernandes, "Economic effects of coronavirus outbreak (COVID-19) on the world economy," available at SSRN 3557504 (2020).
- <sup>15</sup>O. Coibion, Y. Gorodnichenko, and M. Weber, "Labor markets during the COVID-19 crisis: A preliminary view," Technical Report, National Bureau of Economic Research, 2020.
- <sup>16</sup>N. Cellini, N. Canale, G. Mioni, and S. Costa, "Changes in sleep pattern, sense of time and digital media use during COVID-19 lockdown in Italy," *J. Sleep Res.* **29**, e13074 (2020).
- <sup>17</sup>H. A. Rothan and S. N. Byrareddy, "The epidemiology and pathogenesis of coronavirus disease (COVID-19) outbreak," *J. Autoimmun.* **109**, 102433 (2020).
- <sup>18</sup>N. Chintalapudi, G. Battineni, and F. Amenta, "COVID-19 disease outbreak forecasting of registered and recovered cases after sixty day lockdown in Italy: A data driven model approach," *J. Microbiol. Immunol. Infect.* **53**, 396–403 (2020).
- <sup>19</sup>M. Gatto, E. Bertuzzo, L. Mari, S. Miccoli, L. Carraro, R. Casagrandi, and A. Rinaldo, "Spread and dynamics of the COVID-19 epidemic in Italy: Effects of emergency containment measures," *Proc. Natl. Acad. Sci. U.S.A.* **117**, 10484–10491 (2020).
- <sup>20</sup>J. Roux, C. Massonnaud, and P. Crépey, "COVID-19: One-month impact of the French lockdown on the epidemic burden," *medRxiv* 2020.04.22.20075705 (2020).
- <sup>21</sup>L. Di Domenico, G. Pullano, C. E. Sabbatini, P.-Y. Boëlle, and V. Colizza, "Expected impact of lockdown in Ile-de-France and possible exit strategies," *medRxiv* 2020.04.13.20063933 (2020).
- <sup>22</sup>B. Ghoshal and A. Tucker, "Estimating uncertainty and interpretability in deep learning for coronavirus (COVID-19) detection," *arXiv:2003.10769* (2020).
- <sup>23</sup>T. Hale, A. Petherick, T. Phillips, and S. Webster, "Variation in government responses to COVID-19," Blavatnik School of Government Working Paper 31, 2020.
- <sup>24</sup>R. Li, S. Pei, B. Chen, Y. Song, T. Zhang, W. Yang, and J. Shaman, "Substantial undocumented infection facilitates the rapid dissemination of novel coronavirus (SARS-CoV2)," *Science* **368**, 489–493 (2020).
- <sup>25</sup>R. Nunes-Vaz, "Visualising the doubling time of COVID-19 allows comparison of the success of containment measures," *Global Biosecur.* **1**, 1–4 (2020).
- <sup>26</sup>A. N. Desai, M. U. Kraemer, S. Bhatia, A. Cori, P. Nouvellet, M. Herringer, E. L. Cohn, M. Carrion, J. S. Brownstein, L. C. Madoff *et al.*, "Real-time epidemic forecasting: Challenges and opportunities," *Health Secur.* **17**, 268–275 (2019).
- <sup>27</sup>D. Faranda, I. P. Castillo, O. Hulme, A. Jezequel, J. S. W. Lamb, Y. Sato, and E. L. Thompson, "Asymptotic estimates of SARS-CoV-2 infection counts and their sensitivity to stochastic perturbation," *Chaos* **30**, 051107 (2020).
- <sup>28</sup>J. O. Lloyd-Smith, S. J. Schreiber, P. E. Kopp, and W. M. Getz, "Superspreading and the effect of individual variation on disease emergence," *Nature* **438**, 355–359 (2005).
- <sup>29</sup>F. Brauer, "Compartmental models in epidemiology," in *Mathematical Epidemiology* (Springer, 2008), pp. 19–79.
- <sup>30</sup>T. Alberti and D. Faranda, "On the uncertainty of real-time predictions of epidemic growths: A COVID-19 case study for China and Italy," *Commun. Nonlinear Sci. Numer. Simul.* **90**, 105372 (2020).
- <sup>31</sup>G. Consolini and M. Materassi, "A stretched logistic equation for pandemic spreading," *Chaos Soliton. Fract.* **140**, 110113 (2020).
- <sup>32</sup>F. D'Emilio and N. Winfield, "Italy blasts virus panic as it eyes new testing criteria," ABC News, 2020.
- <sup>33</sup>K. Arin, "Drive-thru clinics, drones: Korea's new weapons in virus fight," The Korea Herald, 2020.
- <sup>34</sup>P. P. AGI, "Come vanno letti i dati sul coronavirus in Italia," AGI Agenzia Italia, 2020.
- <sup>35</sup>L. Ferrari, G. Gerardi, G. Manzi, A. Micheletti, F. Nicolussi, and S. Salini, "Modelling provincial COVID-19 epidemic data in Italy using an adjusted time-dependent SIRD model," *arXiv:2005.12170* (2020).
- <sup>36</sup>J. Cohen and K. Kupferschmidt, "Countries test tactics in 'war' against COVID-19," *Science* **367**(6484), 1287–1288 (2020).
- <sup>37</sup>J. H. Tanne, E. Hayasaki, M. Zastrow, P. Pulla, P. Smith, and A. G. Rada, "Covid-19: How doctors and healthcare systems are tackling coronavirus worldwide," *BMJ* **368**, m1090 (2020).
- <sup>38</sup>P. Kellam and W. Barclay, "The dynamics of humoral immune responses following SARS-CoV-2 infection and the potential for reinfection," *J. Gen. Virol.* **101**, jgv001439 (2020).
- <sup>39</sup>A. T. Xiao, C. Gao, and S. Zhang, "Profile of specific antibodies to SARS-CoV-2: The first report," *J. Infect.* **81**, 147–178 (2020).
- <sup>40</sup>A. Grifoni, D. Weiskopf, S. I. Ramirez, J. Mateus, J. M. Dan, C. R. Moderbacher, S. A. Rawlings, A. Sutherland, L. Premkumar, R. S. Jadi *et al.*, "Targets of T cell responses to SARS-CoV-2 coronavirus in humans with COVID-19 disease and unexposed individuals," *Cell* **181**, 1489–1501 (2020).
- <sup>41</sup>L. Ni, F. Ye, M.-L. Cheng, Y. Feng, Y.-Q. Deng, H. Zhao, P. Wei, J. Ge, M. Gou, X. Li *et al.*, "Detection of SARS-CoV-2-specific humoral and cellular immunity in COVID-19 convalescent individuals," *Immunity* **52**, 971–977 (2020).
- <sup>42</sup>S. M. Kissler, C. Tedijanto, E. Goldstein, Y. H. Grad, and M. Lipsitch, "Projecting the transmission dynamics of SARS-CoV-2 through the postpandemic period," *Science* **368**, 860–868 (2020).
- <sup>43</sup>J. T. Wu, K. Leung, and G. M. Leung, "Nowcasting and forecasting the potential domestic and international spread of the 2019-NCOV outbreak originating in Wuhan, China: A modelling study," *Lancet* **395**, 689–697 (2020).
- <sup>44</sup>L. Peng, W. Yang, D. Zhang, C. Zhuge, and L. Hong, "Epidemic analysis of COVID-19 in China by dynamical modeling," *arXiv:2002.06563* (2020).
- <sup>45</sup>S. A. Lauer, K. H. Grantz, Q. Bi, F. K. Jones, Q. Zheng, H. R. Meredith, A. S. Azman, N. G. Reich, and J. Lessler, "The incubation period of coronavirus disease 2019 (COVID-19) from publicly reported confirmed cases: Estimation and application," *Ann. Intern. Med.* **172**, 577–582 (2020).
- <sup>46</sup>E. Lavezzo, E. Franchin, C. Ciavarella, G. Cuomo-Dannenburg, L. Barzon, C. Del Vecchio, L. Rossi, R. Manganello, A. Loregian, N. Navarin, D. Abate, M. Sciro, S. Meriglano, E. De Canale, M. C. Vanuzzo, V. Besutti, F. Saluzzo, F. Onelia, M. Pacenti, S. G. Parisi, G. Carretta, D. Donato, L. Flor, S. Cocchio, G. Masi, A. Sperduti, L. Cattarino, R. Salvador, M. Nicoletti, F. Caldart, G. Castelli, E. Nieddu, B. Labella, L. Fava, M. Drigo, K. A. M. Gaythorpe, Imperial College COVID-19 Response Team, A. R. Brazzale, S. Toppo, M. Trevisan, V. Baldo, C. A. Donnelly, N. M. Ferguson, I. Dorigatti, and A. Crisanti, "Suppression of a SARS-CoV-2 outbreak in the Italian municipality of Vo'," *Nature* **584**(7821), 425–429 (2020).
- <sup>47</sup>L. F. Olsen and W. M. Schaffer, "Chaos versus noisy periodicity: Alternative hypotheses for childhood epidemic," *Science* **249**, 499–504 (1990).

- <sup>48</sup>H. Andersson and T. Britton, *Stochastic Epidemic Models and Their Statistical Analysis* (Springer Science & Business Media, 2012), Vol. 151.
- <sup>49</sup>J. Dureau, K. Kalogeropoulos, and M. Baguelin, “Capturing the time-varying drivers of an epidemic using stochastic dynamical systems,” *Biostatistics* **14**, 541–555 (2013).
- <sup>50</sup>J. A. Polonsky, A. Baidjoe, Z. N. Kamvar, A. Cori, K. Durski, W. J. Edmunds, R. M. Eggo, S. Funk, L. Kaiser, P. Keating *et al.*, “Outbreak analytics: A developing data science for informing the response to emerging pathogens,” *Philos. Trans. R. Soc. B* **374**, 20180276 (2019).
- <sup>51</sup>G. Viceconte and N. Petrosillo, “COVID-19 R<sub>0</sub>: Magic number or conundrum?,” *Infect. Dis. Rep.* **12**(1), 8516 (2020).
- <sup>52</sup>I. Kashnitsky, “COVID-19 in unequally ageing European regions,” *World Dev.* **136**, 105170 (2020).
- <sup>53</sup>D. Faranda and S. Vaienti, “Extreme value laws for dynamical systems under observational noise,” *Physica D* **280**, 86–94 (2014).
- <sup>54</sup>D. Faranda, Y. Sato, B. Saint-Michel, C. Wiertel, V. Padilla, B. Dubrulle, and F. Daviaud, “Stochastic chaos in a turbulent swirling flow,” *Phys. Rev. Lett.* **119**, 014502 (2017).
- <sup>55</sup>J. Zhang, M. Litvinova, W. Wang, Y. Wang, X. Deng, X. Chen, M. Li, W. Zheng, L. Yi, X. Chen *et al.*, “Evolving epidemiology and transmission dynamics of coronavirus disease 2019 outside Hubei province, China: A descriptive and modelling study,” *Lancet Infect. Dis.* **20**, 793–802 (2020).
- <sup>56</sup>J. A. Al-Tawfiq and A. J. Rodriguez-Morales, “Super-spreading events and contribution to transmission of MERS, SARS, and COVID-19,” *J. Hospital Infection* **105**(2), 111–112 (2020).
- <sup>57</sup>A. Deslandes, V. Berti, Y. Tandjaoui-Lambotte, C. Allou, E. Carbonnelle, J. Zahar, S. Brichler, and Y. Cohen, “SARS-CoV-2 was already spreading in France in late December 2019,” *Int. J. Antimicrob. Agents* **55**, 106006 (2020).
- <sup>58</sup>G. Pullano, E. Valdano, N. Scarpa, S. Rubrichi, and V. Colizza, “Population mobility reductions during COVID-19 epidemic in France under lockdown,” *medRxiv* 2020.05.29.20097097 (2020).
- <sup>59</sup>H. Salje, C. T. Kiem, N. Lefrancq, N. Courtejoie, P. Bosetti, J. Paireau, A. Andronico, N. Hoze, J. Richet, C.-L. Dubost *et al.*, “Estimating the burden of SARS-CoV-2 in France,” *Science* **369**, 208–211 (2020).
- <sup>60</sup>H. Salje, C. Tran Kiem, N. Lefrancq, N. Courtejoie, P. Bosetti, J. Paireau, A. Andronico, N. Hozé, J. Richet, C.-L. Dubost, Y. Le Strat, J. Lessler, D. Levy-Bruhl, A. Fontanet, L. Opatowski, P.-Y. Boelle, and S. Cauchemez, “Estimating the burden of SARS-CoV-2 in France,” *Science* **369**, 208–211 (2020).
- <sup>61</sup>M. Maleki, M. R. Mahmoudi, D. Wraith, and K.-H. Pho, “Time series modelling to forecast the confirmed and recovered cases of COVID-19,” *Travel Med. Infect. Dis.* **37**, 101742 (2020).
- <sup>62</sup>“Coronavirus milano, la 41enne con la febbre il 22 dicembre: ‘ora hanno trovato gli anticorpi al COVID’,” *Corriere della Sera* (April 20, 2020).
- <sup>63</sup>S. Flaxman, S. Mishra, A. Gandy, H. Unwin, H. Coupland, T. Mellan, H. Zhu, T. Berah, J. Eaton, P. Perez Guzman, and N. Schmit, “Report 13: The impact of non-pharmaceutical interventions on COVID-19 in 11 European countries,” *Imperial College report* (2020).
- <sup>64</sup>G. De Natale, V. Ricciardi, G. De Luca, D. De Natale, G. Di Meglio, A. Ferragamo, V. Marchitelli, A. Piccolo, A. Scala, R. Somma, E. Spina, and C. Troise, “The COVID-19 infection in Italy: A statistical study of an abnormally severe disease,” *J. Clin. Med.* **9**, 1564 (2020).
- <sup>65</sup>L. Wang and X. Li, “Spatial epidemiology of networked metapopulation: An overview,” *Chin. Sci. Bull.* **59**, 3511–3522 (2014).
- <sup>66</sup>Q.-X. Long, B.-Z. Liu, H.-J. Deng, G.-C. Wu, K. Deng, Y.-K. Chen, P. Liao, J.-F. Qiu, Y. Lin, X.-F. Cai *et al.*, “Antibody responses to SARS-CoV-2 in patients with COVID-19,” *Nat. Med.* **26**(6), 845–848 (2020).
- <sup>67</sup>Y. Liu, R. M. Eggo, and A. J. Kucharski, “Secondary attack rate and superspread-ing events for SARS-CoV-2,” *Lancet* **395**, e47 (2020).
- <sup>68</sup>A. d’Onofrio, P. Manfredi, and E. Salinelli, “Vaccinating behaviour, information, and the dynamics of sir vaccine preventable diseases,” *Theor. Popul. Biol.* **71**, 301–317 (2007).
- <sup>69</sup>S. Khajanchi, K. Sarkar, J. Mondal, and M. Perc, “Dynamics of the COVID-19 pandemic in India,” *arXiv:2005.06286* (2020).
- <sup>70</sup>M. Renardy, M. Eisenberg, and D. Kirschner, “Predicting the second wave of COVID-19 in Washtenaw county, MI,” *J. Theor. Biol.* **507**, 110461 (2020).
- <sup>71</sup>B. Ghanbari, “On forecasting the spread of the COVID-19 in Iran: The second wave,” *Chaos Soliton. Fract.* **140**, 110176 (2020).
- <sup>72</sup>J. Daunizeau, R. Moran, J. Brochard, J. Mattout, R. Frackowiak, and K. Friston, “Modelling lockdown-induced secondary COVID waves in France,” *medRxiv* 2020.06.24.20139444 (2020).
- <sup>73</sup>E. Dong, H. Du, and L. Gardner, “An interactive web-based dashboard to track COVID-19 in real time,” *Lancet Infect. Dis.* (published online 2020).